Defence Science Journal, Vol 42, No 4, October 1992, pp 265-272


# Sizing Procedures for a Fibre-Reinforced Plastic Box

K. Kamal

*Research and Development Establishment (Engrs), Pune–411 015*

**ABSTRACT**

A fibre-reinforced plastic (FRP) box is an important class of structural component employed as the bending, torsion, or bending-torsion load bearing member in the modern light-weight structures. This paper presents various steps involved in the design of such a box beginning with preliminary analysis and optimization to the final sizing. The box made up of carbon fibre composite is a typical numerical example of such FRP construction. Numerical results obtained from the static stress analysis, the panel buckling analysis and the structural optimization as used for this sizing exercise, are presented. It is believed that the complete procedure of analysis using finite element method and then sizing of any FRP box in a comprehensive way, is reported for the first time.

## 1. INTRODUCTION

Sizing of any structural component is an ultimate task which should be performed by a designer as efficiently and accurately as possible. In most of the situations, the analysis of complete structural assembly becomes essential for the requirements of appropriate simulation of the actual boundary conditions and to include the structural continuity effects on the numerical values of the design stresses required in sizing of a structural component. Therefore, in the sizing of any fibre-reinforced plastic (FRP) composite box, the state of stresses developed in the box is obtained from the analysis of the entire structure of which the box is a basic component, with the simulated boundary conditions and appropriate loading. An aft box used in the aircraft lifting surface could be considered as one of the applications of the FRP multibox construction and, therefore, is taken here as a typical representative numerical example for sizing. Each box in any multibox construction is formed by top and bottom skins of the layered composite FRP materials, supported generally either on a full depth foam or a honeycomb core, or on a framework of spars and ribs. While the design of the foam or honeycomb core type support is mainly accomplished on the selection of its suitable density, the spars and ribs in a framework type of supports, fabricated either as co-cured or co-bonded or co-cured-co-bonded with skin need be sized appropriately.

Structural components made of light-weight laminated fibre-reinforced plastic composite are being used extensively in aerospace, and marine structures. Minimisation of weight by modification of the shape through any mathematical approach invariably involves a number of analysis and design procedures and it becomes essential to develop complete steps of analysing and sizing of FRP constructions used in a fighter aircraft in particular and other structures of field combat in general. The present work is an important effort in this direction.

## 2. CONFIGURATION

The cross-section of the spars or ribs considered here for sizing consists of shear webs and top and bottom flanges. Figure 1 gives the line diagram of a multibox type supporting frame for a typical lifting surface, indicating the location of the box identified for this sizing exercise. The various steps involved in the

Received 2 January 1992, revised 15 May 1992

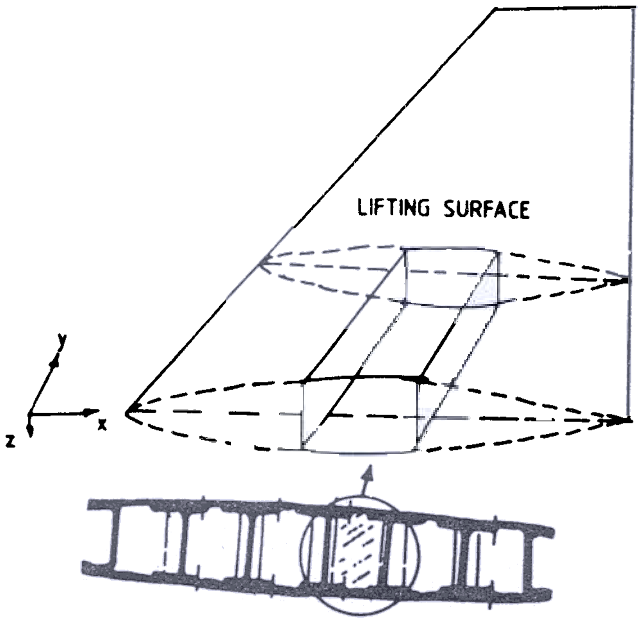


Figure 1. Typical box construction of a lifting surface.

process, beginning from analysis and design phases through panel buckling and structural optimisation to the final sizing of the components are described here.

### 3. PHASE I : PRELIMINARY DESIGN AND STATIC STRESS ANALYSIS

Any sizing exercise starts with the final selection of the plan form geometry of the structure. This is generally done by considering the functional requirements; and in case of a lifting surface, it should be done in conformity with the aerodynamic wind tunnel test results. The identification of the critical load cases, the appropriate location and the types of boundary conditions are done at this stage. After arriving at a final geometrical plan form with the help of the designer's institution, the lifting surface is then considered for analysis.

In the example under consideration, one half of the structure about the plane at the zero aerofoil thickness of the lifting surface is considered due to symmetry in its geometry. First set of numerical data is then generated by analysing the complete lifting surface using a standard finite element software package, such as SAP, NASTRAN, ASKA, or ELFINI. Appropriate numbers, locations and types of the support points to the main structure are decided by several trial

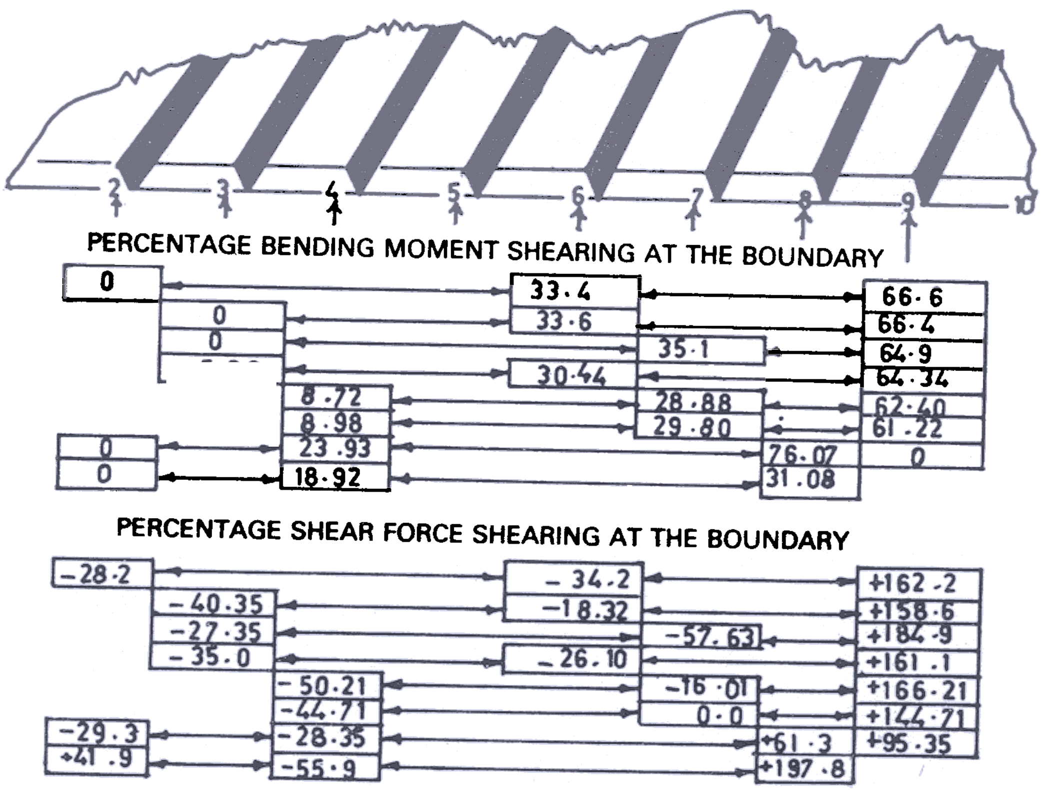


Figure 2. Study of the location and type of boundary conditions.

computations for an assumed uniformly distributed load, and the most suitable one is selected based on the designer's intuition. These results for different locations at its bottom ribs are given in Fig. 2. At this stage of calculations, the composite skin with uniform initial thickness of commonly used [0/±45/90] layups is considered. Zero degree fibre, oriented at the same angle is also assumed at this stage. The best trial orientation of the zero degree fibre is by keeping it along the main spar orientation. The skin is idealised using layered anisotropic finite elements. The webs are idealised as single thickness shear elements of the precalculated equivalent orthotropic properties. The flanges of the ribs and the spars are idealised using the equivalent lumped area bars. To obtain the numerical values of a set of design stresses in the skins, the webs and the flanges of the structure, uniformly distributed pressure is used initially in the absence of other load data. Then the static analysis runs are made under the three critical load distributions identified by aerodynamic wind tunnel test. This distribution at the tip of the aft box is shown in Fig. 3, where $\beta$, the side slip angle and $\delta$, the control surface deflection are the parameters used in aerodynamic load calculations. Three additional sets of numerical values of the stresses and their directions are then obtained.

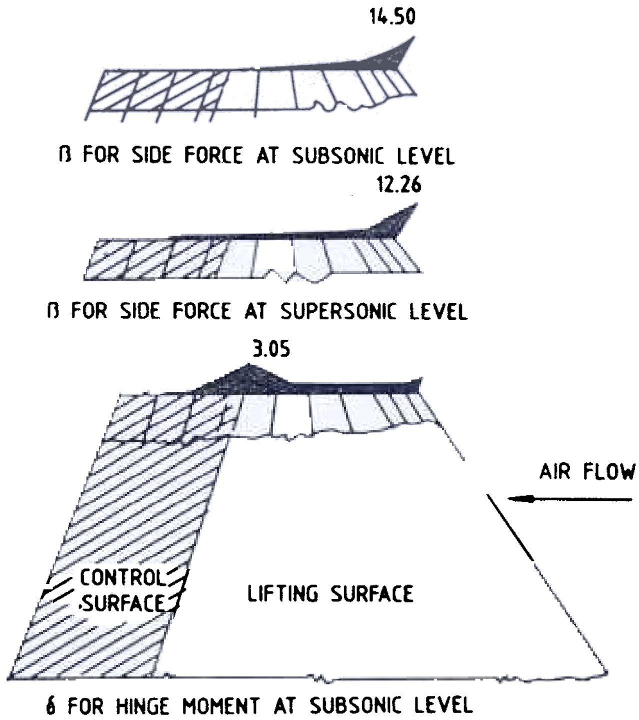


Figure 3. Load distribution at the tip of the aft box.

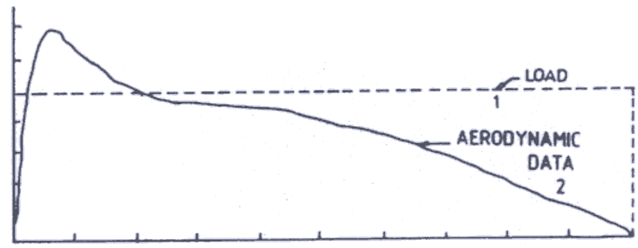


Figure 4. Effect of change in the loading pattern.

Subsequently, the effect of change in the stress and deflection values due to the change in loading patterns is studied to ascertain the percentage difference in the numerical values obtained while using uniformly distributed load, as in Fig. 4, is given in Table 1. By comparing these results with the design allowable, the boundaries of the skin thickness variations are marked and various constant thickness zones, needed for optimization, are identified as shown in Fig. 5. The direction of zero degree fibre is also correctly oriented at this stage so as to follow the direction of the principal stresses. For the sake of completeness, static re-runs are made to study the effect of the change in fibre orientation on the result, and the most optimal one is considered for further analysis as marked in Fig. 6. All these results thus obtained form the appropriate input

Table 1. Comparison of different load cases

| Case | Shear force and bending moment | | | | Displacement | Stresses | | |
|---|---|---|---|---|---|---|---|---|
| | | S (%) | M (%) | M (%) | (cm) | $\sigma X$ | $\sigma Y$ | $\sigma XY$ |
| 1. UDL | BM | – | 40.16 | 59.84 | 12.53 | 0.149 | –6.235 | –1.424 |
| | SF | 55.9 | –8.47 | 147.42 | | | | |
| 2. Load | BM | – | 43.14 | 56.86 | 10.16 | 0.125 | –4.791 | –0.998 |
| | SF | 42.5 | –21.83 | 120.74 | | | | |

BM: bending moment; SF: shearing force

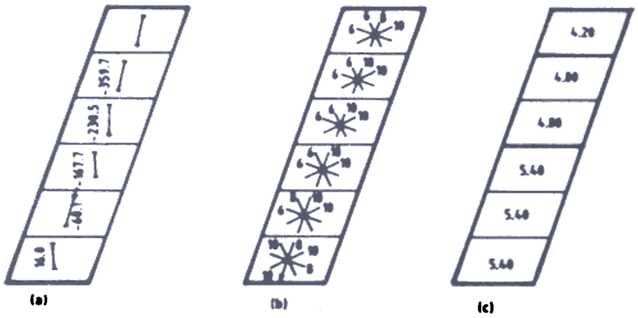

Figure 5. Initial input data for the box skin.

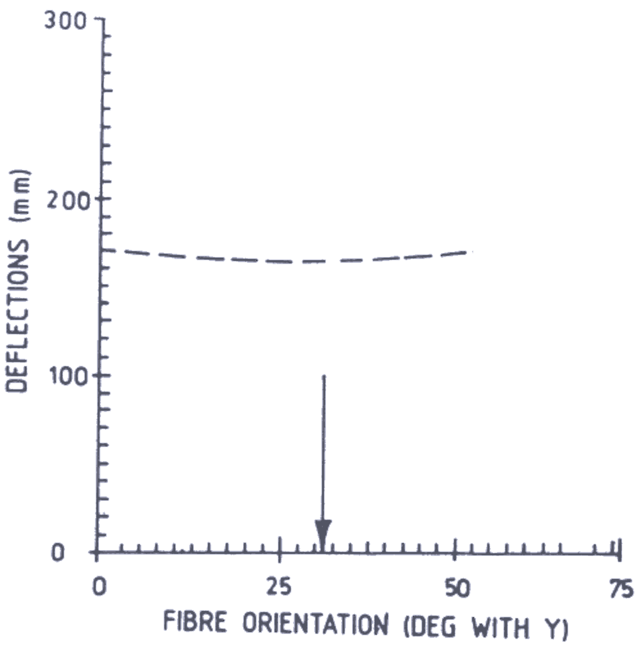


Figure 6. Study of the effect of change in zero degree fibre orientation.

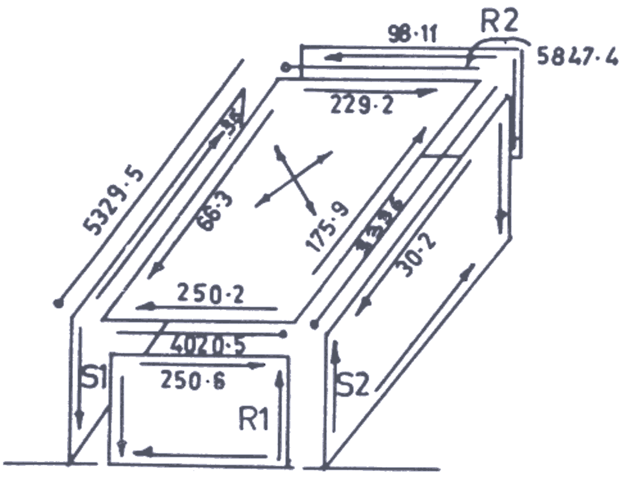


Figure 7. Maximum state of stresses in the box.

data for any sizing exercise. The static stress flow values and their directions are recomputed with these updated inputs. The maximum stresses and the maximum axial forces developed in the members under different load cases along with the directions of principal flows are then picked up as reported in Fig. 7 and are used in subsequent phases.

## 4. PHASE II : PANEL BUCKLING UNDER COMBINED AND INDIVIDUAL LOADS

Panel buckling plays an important role in the sizing of any structural component. Often a structural failure is dictated by buckling rather than the strength of the material. In the literature, several standard data sheets are available to evaluate the buckling strength of the panel made up of metallic material under pure shear, pure bending and the combination of shear and bending loads. However, due to the various possible permutations and combinations that the composite materials offer in terms of the layup sequence in a panel, it becomes rather difficult to compile single data sheet unlike that in the case of metallic materials. In the absence of such data sheets, the designers generally create the required limited data, relevant to the given situation. In this phase the design data pertaining to panel buckling under pure shear and pure bending cases is created. The layup for the carbon fibre composite (CFC) skin panel is described, neglecting the effects of

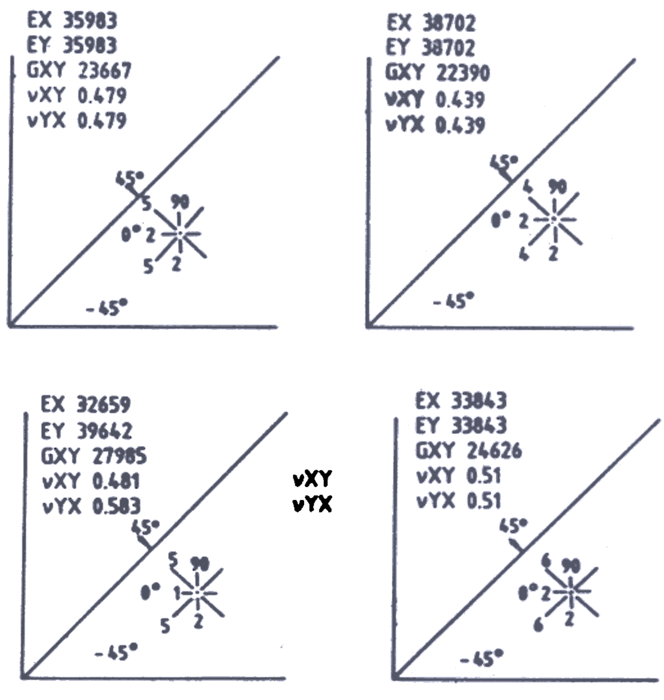


Figure 8. Different trial layups for shear webs.

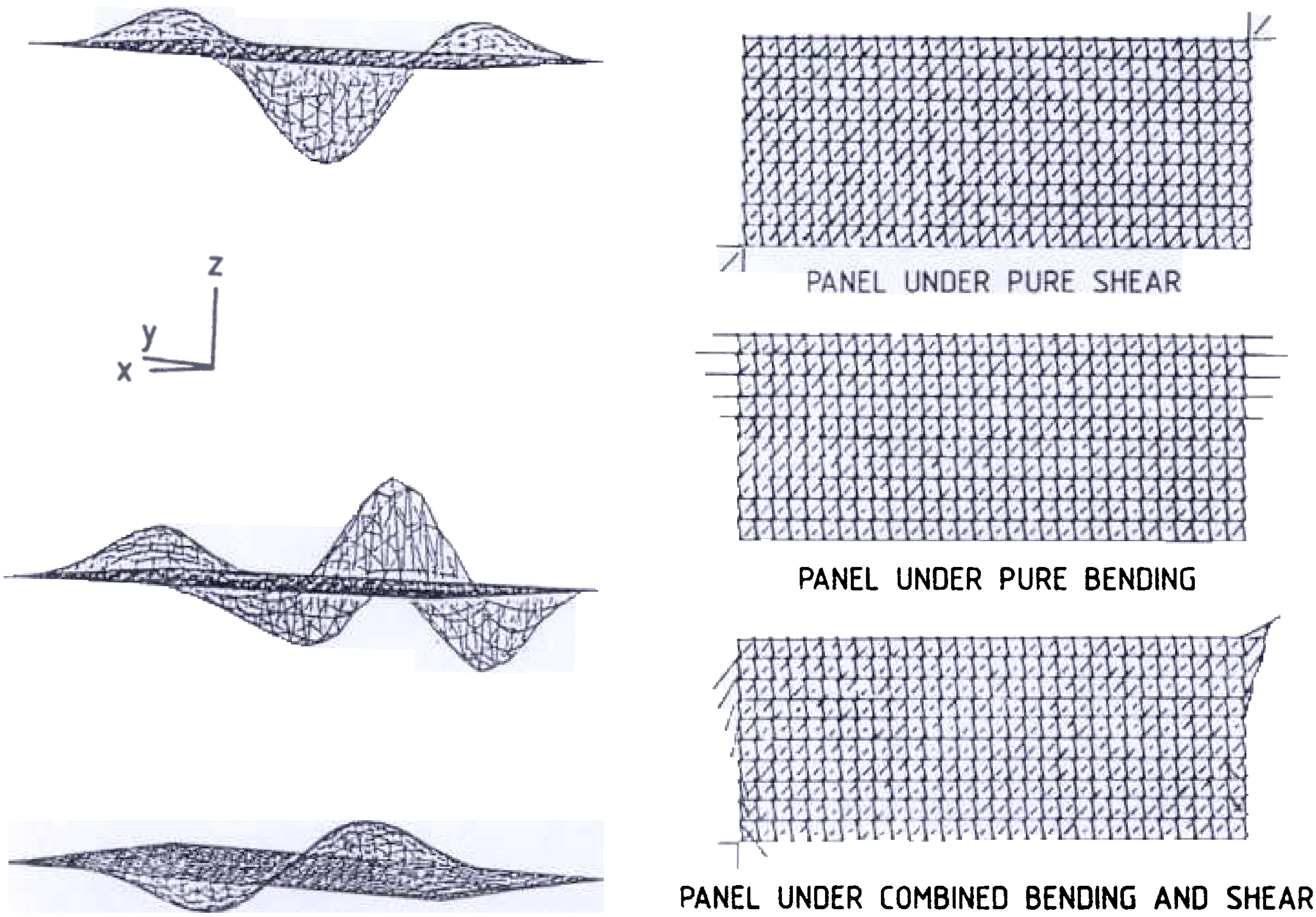


**Figure 9. Buckling analysis showing first buckling modes.**

sequencing in view of small thickness. Four different trial layups are considered for the spar and rib webs as given in Fig. 8. The equivalent orthotropic properties of these layups which were used in Phase I are also given in the figure. The general purpose finite element software ELFINI is used to obtain the buckling solutions. Triangular plate bending elements are used for the idealisation. Simply supported boundary conditions are simulated at the boundary nodes along the edges. Isostatic boundary conditions are applied for the in-plane displacements to suppress the in-plane rigid body displacement. The relevant loading, either pure shear, pure bending or the combination of both, is achieved by applying the appropriate loads on the boundary nodes. The combined stresses induced in the skin and webs, as appropriate under different load cases (as obtained in Phase I) are applied on the panel for the buckling analysis to simulate the actual panel loading conditions.

The panel buckling analysis under individual and combined loading is then carried out for a few laminates representing the skin and shear web panels for the box, respectively. Typical of these data plots are presented in Fig. 9. To study the effect of panel dimensions on the buckling parameter, different panel aspect ratios are considered and these results are plotted and a typical of these plots is shown in Fig. 10.

## 5. PHASE III : STRUCTURAL OPTIMIZATION

Sizing of the structural box used in any lifting surface is influenced by aeroelastic control efficiencies in addition to the static load distributions. The optimization study of this structure should, therefore, include such effects. Structural optimization is carried out for the entire lifting surface, with its supporting frame structure dimensions as the fixed quantities and the individual layer thickness of the top and bottom skins as the design variables. This is because the skin of this box structure resists most of the combined state of direct and shear stresses due to bending and torsional loads. Whereas, the supporting structure design is mainly dependent only on the shear flows due to bending and torsional loads. The objective function in this optimization, therefore, is the skin weight. The structural optimization is carried out for the entire surface including the load transfer due to a control surface hinged on the rear spar at suitable locations. The stress, buckling, aeroelastic control efficiencies and the various anticipated technological constraints are used in this optimization. Standard finite element software with optimization capability is used for this purpose. At the end of each iteration of the optimization calculations, a new finite element mesh is generated using the optimum values of the design variables so obtained.

A convergence study on the values of design variables and the objective function showed that the converged optimal solution is reached at the fifth iteration. The optimized total thickness and the number of layers in each direction is thus obtained for the top and bottom skins. The stress and buckling analysis, i.e., from Phase I to Phase III are then repeated till no change is noticed in the final results for the skin over the identified box (Fig. 11). Results for the entire lifting surface, obtained during optimization showing the effects of variations in various design parameter values on the objective function are given in Table 2.

**Table 2. Optimization results for the lifting surface**

| Parameter used | Constraints | | | | | |
|---|---|---|---|---|---|---|
| | Stress alone | Buck alone | Stress + buck | Stress + aero | Stress + aero+buck | Stress+aero +buck+tech |
| Weight at starting | 18.099 | 18.099 | 18.099 | 18.099 | 18.099 | |
| Weight after optimisation | 6.439 | 10.120 | 10.347 | 11.247 | 12.703 | |

| Parameter used | Number of spars | | |
|---|---|---|---|
| | F(5) | F(6) | F(7) |
| Weight at starting | 18.021 | 18.021 | 18.021 |
| Weight after optimisation | 14.530 | 12.879 | 12.811 |

| Parameter used | Reference axis of 0° | | | | |
|---|---|---|---|---|---|
| | 35° | 30° | 25° | 20° | 15° |
| Weight at starting | 18.021 | 18.021 | 18.021 | 18.021 | 18.021 |
| Weight after optimisation | 12.077 | 12.384 | 11.933 | 11.555 | 11.253 |

| Parameter used | Case 1 | Case 2 | Case 3 |
|---|---|---|---|
| Weight at starting | 18.099 | 18.021 | 18.099 |
| Weight after optimization | 12.728 | 12.786 | 13.319 |

Case 1 : Use of full depth honeycomb
Case 2 : Use of honeycomb with frame
Case 3 : Use of frame of spars and ribs

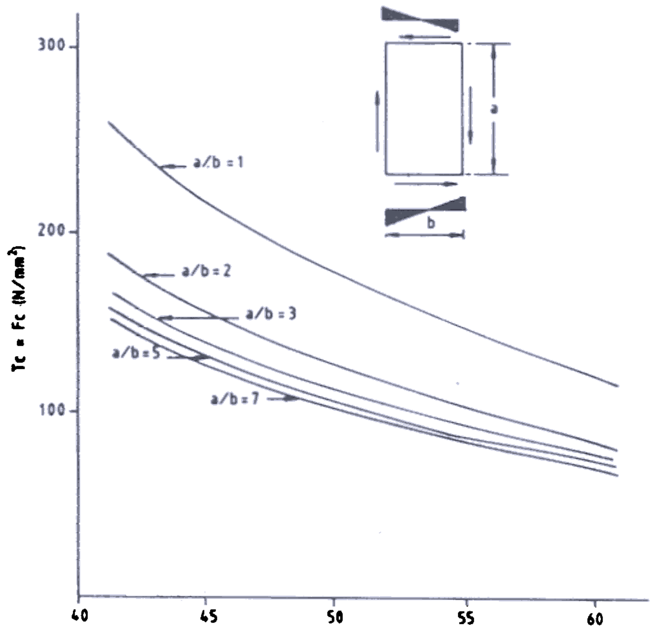


**Figure 10. Buckling values for an example case.**

## 6. PHASE IV : SIZING OF THE SKIN AND THE SUPPORTING FRAME STRUCTURE

As the bending and torsional characteristics are basically dictated by the stiffness offered by CFC skins

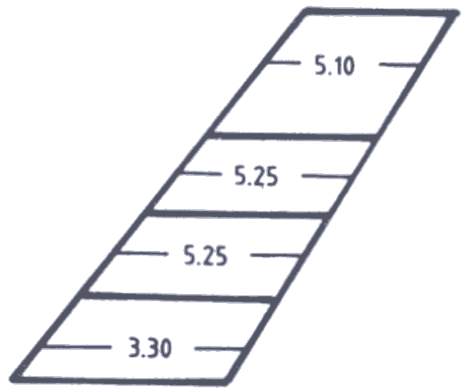


**Figure 11. Optimization results for the skin over the box.**

of the aft box, at the end of the optimization phase, the sizing of top and bottom skins of the box in terms of layups and total thicknesses is completed. These results are shown in Fig. 11. The elements of the supporting structure, i.e., spars and ribs mainly contribute in the transfer of the shear. The size assigned to the element of the structure in Phase I to Phase III was mainly based on some preliminary calculations and the intuition of the designers. Having successfully completed the studies up to Phase III, it is essential to do a round of resizing of the supporting structure

**Table 3. Sizing of the members under shear loads**

| Member ID | Layups used 0°/45°-45°/90° (CFC fibre) | Max. shear flow Values (N/mm) | | | Max. shear flow (N/mm) | Allow. shear stress (N/sq mm) | Thickness required for shear (mm) | Assumed thickness t (mm) | Shear stress for 't' (N/sq mm) | Shear buckling stress for design thickness | | | | Remarks |
|---|---|---|---|---|---|---|---|---|---|---|---|---|---|---|
| | | Load case 1 | Load case 2 | Load. case 3 | | | | | | KE ($\times 10^4$) | b | $(t/b)^2$ ($\times 10^{-h}$) | $\tau_{cr}$ = KE$(t/b)^2$ | |
| $S_1$ | 1/5/5/2 | 36.4 | 12.30 | 34.8 | 36.4 | 180 | 0.20 | 1.95 | 18.66 | 29.0 | 117.9 | 2.74 | 79.33 | OK |
| $S_2$ | 1/5/5/2 | 28.8 | 17.70 | 30.2 | 30.2 | 180 | 0.17 | 1.95 | 15.48 | 29.0 | 121.5 | 2.58 | 74.70 | OK |
| $R_1$ | 1/5/5/2 | 241.2 | 163.7 | 150.6 | 250.6 | 180 | 1.38 | 2.25 | 111.37 | 43 | 119.6 | 3.5 | 152 | OK |
| $R_2$ | 1/5/5/2 | 98.11 | 55.5 | 84.3 | 98.11 | 180 | 0.54 | 1.65 | 59.5 | 43 | 100 | 2.7 | 117.0 | OK |

**Table 4. Sizing of the members under combined bending and shear**

| Member ID | Layups used 0°/45°/-45°/90° (CFC fibre) | Max value of axial forces in flangs (N) | | | | Max bending stress | | Critical bending stress (N/sq mm) | | | | | $\frac{fb}{fcr}$ | | | $\tau/\xi$ | $fb/fcr + (\tau/\xi r)^2$ | Remarks |
|---|---|---|---|---|---|---|---|---|---|---|---|---|---|---|---|---|---|---|
| | | Load case 1 | Load case 2 | Load case 3 | $F_{max}$ | Area (sqmm) | fb N/sqmm | t mm | b mm | t/b | KE $\times 10^4$ | fcr=KE $(t/b)^2$ | | | | | | |
| $S_1$ | 1/5/5/2 | 3984 | 5330 | 4374 | 5330 | 40 | 133.2 | 1.95 | 117.9 | 0.017 | 135 | 390.15 | 0.34 | 18.7 | 79.3 | 0.24 | 0.39 | OK |
| $S_2$ | 1/5/5/2 | 2930 | 3336 | 3210 | 3336 | 40 | 33.41 | 1.95 | 121.5 | 0.016 | 135 | 345.60 | 0.24 | 15.4 | 74.7 | 0.21 | 0.28 | OK |
| $R_1$ | 1/5/5/2 | 3936.0 | 3718.3 | 4020.5 | 4020.5 | 100 | 40.2 | 1.95 | 119.6 | 0.0163 | 150 | 395.5 | 0.101 | 111.4 | 152.9 | 0.73 | 0.83 | OK |
| $R_2$ | 1/5/5/2 | 3352.6 | 5847.4 | 3070.9 | 5847.4 | 75 | 78.0 | 1.95 | 100.0 | 0.019 | 150 | 570.0 | 0.136 | 59.5 | 117.6 | 0.51 | 0.39 | OK |

elements, mainly the webs, based on the maximum stress flows that are now available from the previous phase. The numerical calculations using these design stresses developed in the member for shear loads are compared with the allowable and are shown in Table 3. The results of final sizing calculations for combined bending and shear are reported in Table 4.

## 7. CONCLUSION

The complete procedure of analysing and designing of an FRP box using finite element analysis through structural optimization to sizing of the individual members is reported. It is hoped that this paper will set the procedural guidelines for such sizing exercises for the structural designers.

## ACKNOWLEDGEMENTS

The author is thankful to Shri VK Bakshi and Dr K Shamsundar for providing technical facilities to conduct these studies in India and abroad.